Letter

Bound electron screening effect on ion-ion potential of warm and hot dense matter

Meng Lv,[1] Ke Li,[1,*] Chuan Wang,[1] Ronghao Hu,[1,†] Yang Zhao,[2] and Jiayu Dai[3]

[1]*College of Physics, Sichuan University, Chengdu 610064, People's Republic of China*

[2]*Research Center of Laser Fusion, China Academy of Engineering Physics, P. O. Box 919-986, Mianyang 621900, People's Republic of China*

[3]*Department of Physics, College of Science, National University of Defense Technology, Changsha, Hunan 410073, People's Republic of China*

(Received 21 December 2020; accepted 4 May 2021; published 17 May 2021)

The effects of bound electron screening in warm and hot dense matter are investigated analytically and a theoretical description of screened short-range repulsion is given meanwhile. An empirical ion-ion potential including the classic charge screening and chemical bond attraction at various temperatures and densities is proposed. By solving hypernetted chain equations and comparing the obtained radial distribution function (RDF) with *ab initio* simulations, the proposed ion-ion potential is found to be promising over a wide range of temperatures and densities for warm dense aluminum and iron. The elastic scattering amplitude and the x-ray absorption near the edge structure of warm dense aluminum calculated from the obtained RDF are in good agreement with experiment results.

DOI: 10.1103/PhysRevE.103.L051203

I. INTRODUCTION

Understanding structural properties of warm dense matter (WDM) is of wide interest with application to planetary physics and fusion science. Such conditions are relevant to planetary interiors [1], solids heated with x-ray free electron lasers [2], high-power lasers [3] and laser-driven shocks [4,5], and imploding capsules during inertial confinement fusion [6]. Angularly and spectrally resolved x-ray scattering and diffraction experiments [4,5,7–14] have been carried out on WDM and dense plasma samples with the aim of accessing information on the static and dynamic structure factors. Using the structure of the x-ray absorption edge [3,15–18], one can also extract information on the electronic and structural properties such as radial distribution function (RDF) and local atomic order. The theoretical investigation of WDM is challenging since the interactions of free electrons, bound electrons, nuclei, ions, and neutral particles should be treated accurately. Increasing computing power enables the wide application of the density functional molecular dynamics (DFT-MD) method [19–29], which is aimed to completely describe the interacting quantum systems including strong ionic correlations with quantum effects of free and bound electrons. However, *ab initio* simulations demand much computational power and are subject to limitations concerning temperature, density, and system size. Various reduced models and simulation methods have been developed to reduce the computational cost while retaining sufficient accuracy. The pseudoatom molecular dynamics simulations combines density-functional-theory-based calculations of the electronic structure to classical molecular dynamics simulations with pair-interaction potentials [30,31]. Classical and quantum hypernetted chain (HNC) methods with effective ion-ion potentials from density-functional theory or first-principle simulations has been proven to be an efficient reduced model [19,20,32–37]. The ion-ion interaction potential plays an important role because the ionic structure of WDM can be determined very efficiently by the HNC approach with the effective ion-ion potential. The Yukawa potential model considers only ions that interact via screened Coulomb forces, which leads to large discrepancies for small distance between ions, and the short-range interionic screening plays an important role in determining the static structure factor (SSF) [38]. Wünsch *et al.* [19] and Vorberger *et al.* [37,39] modified the Yukawa potential by adding a short-range repulsion (SRR) potential. The static ion structures calculated from the modified potential are closer to DFT-MD simulations than the Yukawa potential [19,37]. However, difficulties still remain for obtaining accurate RDF structures at low temperatures with the modified ion-ion potential.

In this paper, we further investigate the short-range screening effect of bound electrons on ion-ion potential of warm and hot dense matter. An empirical ion-ion potential including effects of classic charge screening and chemical bond attraction is proposed. By solving HNC equations with the proposed ion-ion potential, the RDF of warm dense aluminum and iron can be obtained numerically. The results agree well with *ab initio* simulations over a wide range of densities and temperatures. Furthermore, elastic scattering amplitude and the x-ray absorption near edge structure (XANES) calculated from the obtained RDF are in good agreement with experiment results.

II. METHODS

RDF or SSF represents statistic distribution of ions in WDM, which can be obtained by solving the HNC equations. The HNC approach involves a closed system of

*Present address: School of Physics, Peking University, Beijing 100871, People's Republic of China.

†Corresponding author: ronghaohu@scu.edu.cn

three equations depending on density, temperature, and the pair-interaction potentials [19,35–37]:

$$\begin{cases} h_{ab}(r) = c_{ab}(r) + \sum_c n_c (h_{ab}(r) * c_{ab}(r)) \\ g_{ab}(r) = \exp[-\beta V_{ab}(r) + h_{ab}(r) - c_{ab}(r)] \\ h_{ab}(r) = g_{ab}(r) - 1. \end{cases} \quad (1)$$

$g_{ab}(r)$ is the RDF, which describes the distribution of particles in the system, $h_{ab}(r)$ is the total correlation function for species a and b containing the direct correlation $c_{ab}(r)$ between these two species and all indirect correlations provided by all other species c [40], $V_{ab}(r)$ is the pair interaction potential function, r is the distance between particles, n_c is the number density of species c and $\beta = \frac{1}{k_B T}$. Both free and bound electrons are treated as arbitrarily degenerate background and only ion species are considered in our model. The HNC equations can be solved numerically through an iterative method [37].

Different from ideal plasma and condensed matter, WDM is partially ionized, strongly correlated, and arbitrarily degenerate. Chemical bonds formed by bound electrons also play important roles in mid-Z and high-Z WDM [37,41]. Chemical bonds in WDM are not stable due to the thermal motions of ions. When two ions get close, chemical bonds can probably be formed and, when the ions separate, the formed bonds are broken [41]. The chemical bonds are more stable for lower densities and temperatures as the conditions are closer to condensed matter. The attraction force of chemical bonds reduces the repulsion force of the ions. Taking into account the classic charge screening and chemical bond attraction, an empirical ion-ion interaction potential including the Yukawa potential and bound electron screened SRR potential can be written as

$$V_{ii}(r) = \left[\frac{(Ze)^2}{r}(1 - e^{-f(r)}) + \frac{(Z_c e)^2}{r} e^{-f(r)} \right] e^{-\kappa r}, \quad (2)$$

where Z and Z_c are the charge number of ion and nucleus, respectively, e is the elementary charge, κ is the inverse screening length of free electrons, and $f(r)$ is the screening function of bound electrons. We use the Yukawa model [20] to calculate the average charge number Z. For arbitrary degenerate systems, the calculation of the inverse screening length κ should consider the full Fermi integrals [42],

$$\kappa = \left[\frac{4\pi}{k_B T} \sum_c e_c^2 \frac{2s_c + 1}{\Lambda_c^3} I_{-1/2}(\beta\mu_c) \right]^{1/2}, \quad (3)$$

where s_c is the spin quantum number of species c and Λ_c is the thermal wavelength defined by $\Lambda_c = (\frac{2\pi\hbar^2}{m_c k_B T})^{1/2}$. $I_{-1/2}(\beta\mu_c)$ is the Fermi integral and can be calculated using the dimensionless quantity $y_c = \frac{n_c \Lambda_c^3}{(2s_c+1)}$:

$$I_{-1/2}(\beta\mu_c) = \begin{cases} \frac{y_c}{(1+0.353y_c - 0.0099y_c^2 + 0.000375y_c^3)} & y_c < 5.5 \\ \frac{y_c^{1/3}}{(0.806 + 0.4535y_c^{-4/3} + 1.7y_c^{-8/3})} & y_c > 5.5. \end{cases} \quad (4)$$

For the HNC method, the quantum nature of the electrons can only be treated approximately. The interaction between ions are repulsive in general, but the attraction induced by chemical bonds can reduce the repulsive force [37]. As the effect of the chemical bond is mainly short-range attraction, an extra screening term can be added to the SRR potential to include the effect of chemical bonds. An empirical formula for the bound electron screening function can be written as

$$f(r) = \frac{ln2}{R_i} r + (\rho_0/\rho)^{5/3} e^{T_0/T}. \quad (5)$$

The first term on the right-hand side of Eq. (5) is the contribution of classic charge screening by bound electrons, R_i is the ion radius and can be computed by [43–45]

$$R_i = \begin{cases} \frac{1.5(n-1)^2 a_0}{0.01Z_c + 1.29Z}, n = 2 \\ \frac{1.5(n-1)^2 a_0}{0.19Z_c + 1.29Z}, n = 3 \\ \frac{1.5(n-1)^2 a_0}{0.5235n^{-0.6746}Z_c + 0.4702\exp(0.3151n)Z}, n > 3. \end{cases} \quad (6)$$

Here n is the maximum principal quantum number of the element at ground state, a_0 is the Bohr radius. The second term on the right-hand side of Eq. (5) is the contribution of chemical bond attraction. ρ_0 and T_0 are the only two free parameters in our model and are kept constant for the same material under all conditions.

The effective ion-ion interaction potential [Eq. (2)] involves the Yukawa potential at the range of long distance and the screened SRR potential in the vicinity of the central ion. The major difference between our potential and the potential of Vorberger *et al.* [37,39] is the addition of an extra screening term due to chemical bond attraction in Eq. (5). For high densities and temperatures, the collision rates between ion-electron and ion-ion are higher and the chemical bonds are less stable. The screening effect of the chemical bond is more important at low densities and temperatures, as implied by Eq. (5).

III. RESULTS AND DISCUSSIONS

The comparison of RDFs calculated from our model and *ab initio* simulations for Al at various densities and temperatures are shown in Fig. 1. $\rho_0 = 3.0218$ g/cm^3 and $T_0 = 605.8$ K are used in Eq. (5) for Al. Figures 1(a)–1(c) show the RDFs of Al at $\rho = 2.7$ g/cm^3 and $T = 1100, 2000, 5000$ K, respectively. The results of our model agree well with *ab initio* quantum molecular dynamics (QMD) simulations especially inside the first coordination shell [3]. The peak value of the RDF decreases as the temperature increases, indicating that short-range order of ions decreases with the increasing of temperature. The properties of the chemical bond between Al ions can be derived from the RDF. The bond length can be estimated by the coordinate of the first peak of the RDF and the coordination number can be calculated as $N = 4\pi\rho \int_0^{r_{\min}} g(r) r^2 dr$, where $r_{\min}$ is the coordinate of the first minimum in the RDF [46]. The bond lengths between Al ions are 5.1, 5.1, 4.9 and the coordination numbers are 13.33, 13.28, 13.09 for $T = 1100, 2000, 5000$ K, respectively. The decreasing of coordination number also implies the short-range order decreases as the temperature increases. Figure 1(d) shows the RDF of Al at $\rho = 3.4$ g/cm^3 and $T = 1.1$ eV. The result of our model are compared with results of DFT-MD simulations and the HNC method with Yukawa plus SRR potential (HNC-Y+a/r^4) [19]. Compared to the result of HNC-Y+a/r^4, our model is closer to the result of DFT-MD simulation in terms of peak values and coordinates.

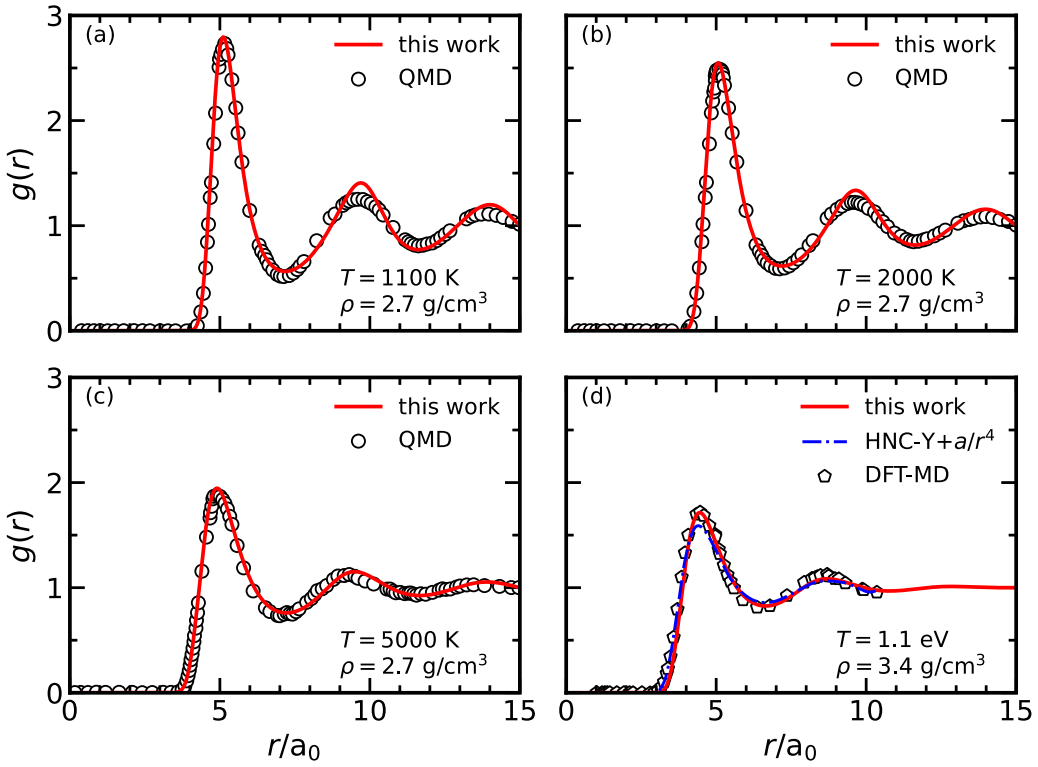

FIG. 1. RDFs of warm dense Al at various densities and temperatures. The QMD simulation results in (a)–(c) are from Ref. [3]. The results of HNC-Y+a/r^4 and DFT-MD in (d) are from Ref. [19]. The charge numbers Z calculated by Yukawa model are 0.207, 0.260, 0.413, and 0.700 in (a)-(d), respectively.

The x-ray elastic scattering amplitude and XANES can be calculated from the RDF of our model for comparison with experimental results. The elastic scattering amplitude $W_R(k) = S_{ii}(k)[f(k) + q(k)]^2$ of x ray with energy of 17.9 keV scattered by Al at $\rho = 8.1$ g/cm^3 and $T = 10$ eV is shown in Fig. 2(a). $S_{ii}(k) = 1 + 4\pi n_i \int_0^\infty [g(r) - 1]\frac{\sin(kr)}{kr} r^2 dr$ is the ion SSF, n_i is the number density of ions. $f(k)$ is the ion form factor and $q(k)$ describes the screening cloud of the free electrons surrounding the ion. $f(k)$ and $q(k)$ can be calculated using the method of Ref. [47]. The scattering amplitude calculated from the RDF of our model matches better with experimental measurements than the HNC-Y+a/r^4 method for $k < 10$ Å^{-1} at the corresponding density and temperature [13]. The x-ray elastic scattering amplitude of Al at ρ=6.3 g/cm^3 and T=1.75 eV calculated with our model is compared with experiment, DFT-MD simulation, and the HNC-Y+a/r^4 data from Ref. [14]. Both our model and the HNC-Y+a/r^4 method are consistent with experiment and DFT-MD simulation as shown in Fig. 2(b). The K-edge XANES can be calculated from the RDF with the multiple-scattering theory in a muffin-tin potential [48,49]. The obtained XANES spectra for Al at various densities and

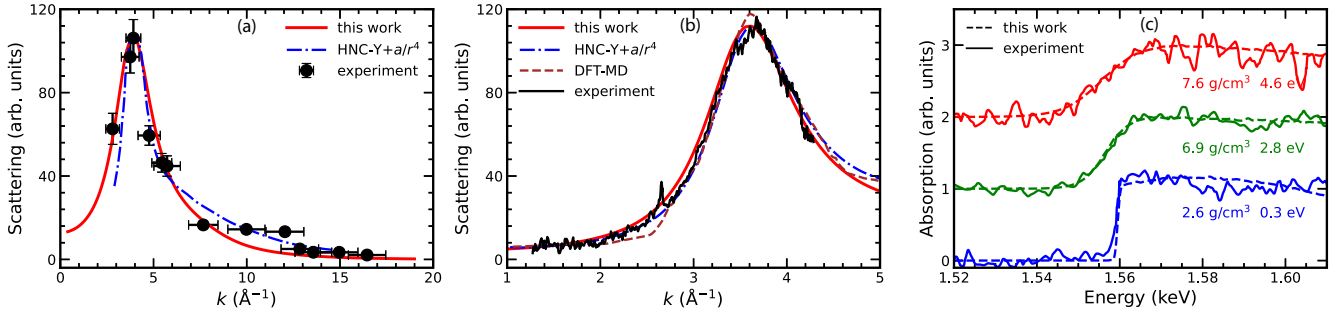

FIG. 2. (a) The elastic scattering amplitude as a function of scattering wave number k for Al at $\rho = 8.1$ g/cm^3 and $T = 10$ eV. The results of experiments and HNC-Y+a/r^4 are from Ref. [13]. (b) The elastic scattering amplitude as a function of scattering wave number k for Al at $\rho = 6.3$ g/cm^3 and $T = 1.75$ eV. The results of experiments, DFT-MD simulation, and HNC-Y+a/r^4 are from Ref. [14]. (c) K-edge XANES of Al at various densities and temperatures. The experimental results are from Ref. [16]. The charge numbers Z calculated by Yukawa model are 2.071 in (a), 1.100 in (b), and 0.344, 1.090, 1.347 for T=0.3, 2.8, 4.6 eV in (c).

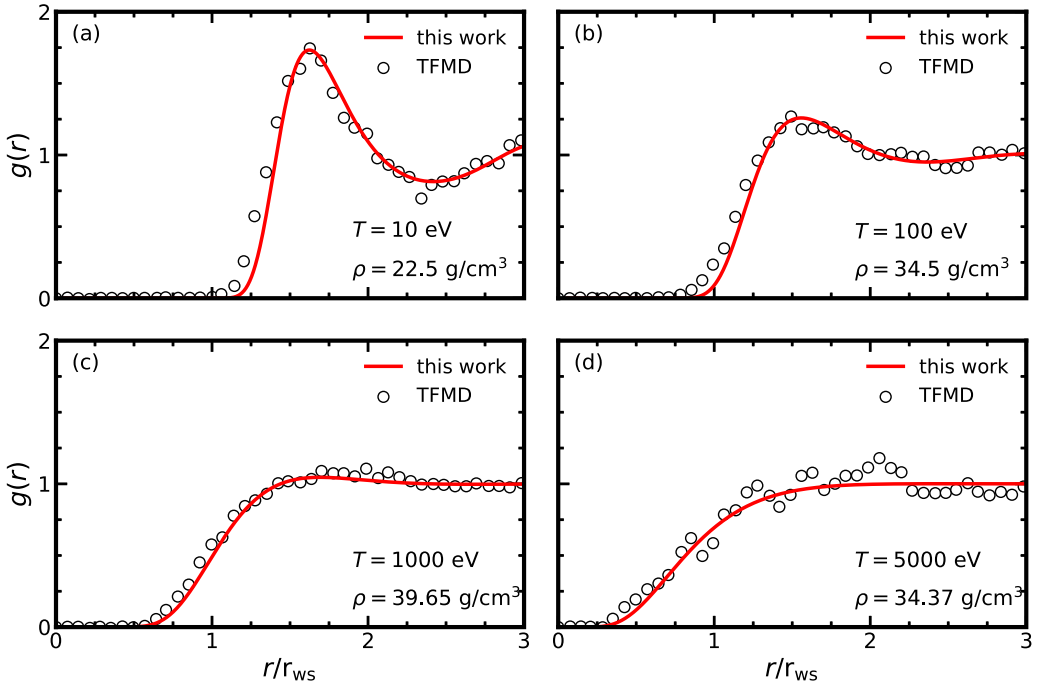

FIG. 3. RDFs of warm and hot dense Fe at various densities and temperatures. The TFMD simulations results in (a)–(d) are from Ref. [21]. $r_{WS} = (3/4\pi n_i)^{1/3}$ is the Wigner-Seitz radius. The charge numbers Z calculated by Yukawa model are 2.11, 6.11, 19.97, and 25.47 in (a)–(d), respectively.

temperatures are shown in Fig. 2(c). The K-edge position and slope of experimental results [16], which are sensitive to density and temperature, can be well reproduced by our model as depicted in Fig. 2(c).

The ionic structure of warm and hot dense iron is also investigated with our model and the results are compared with *ab initio* simulation results. For iron, $\rho_0 = 15.2021$ g/cm^3 and $T_0 = 45\,991.3$ K are used in Eq. (5). The RDFs of warm and hot dense Fe with temperatures from 10 eV to 5000 eV are shown in Fig. 3. With increasing temperature, the short-range order of Fe ions disappears as shown in Figs. 3(a)–3(d) and this trend is correctly reflected by our model as compared to the results of Thomas-Fermi molecular dynamics (TFMD) simulations [21]. The RDFs of warm dense Fe with temperatures fixed at 240 eV and densities from 1.6 to 40 g/cm^3 are shown in Fig. 4. The overall trend of our model is consistent with the results of orbital-free molecular dynamics (OFMD) simulations [20] while the peak values of our model is slightly lower than OFMD results.

IV. CONCLUSIONS

An empirical ion-ion potential of WDM is proposed and validated using the HNC method. The ion-ion potential includes the Yukawa potential and bond electron screened SRR potential. An empirical formula of screening effects including both linear charge screening and chemical bond attraction is given for various densities and temperatures. The RDF obtained from proposed potential is consistent with *ab initio* simulations for warm dense Al and Fe at various densities and temperatures. The elastic scattering amplitude and XANES calculated from the obtained RDF for Al are in good agreement with experiment results. The presented comparisons between results of our model and results of *ab initio* simulations and experiments demonstrate the capability of our model for obtaining the structural information of warm and hot dense matter in a relatively wide temperature and density range. With the inclusion of linear screening and chemical bond attraction effects on SRR potential, our model shows better consistency with *ab initio* simulations and experiments than the HNC-Y+a/r^4 approach. The free parameters ρ_0 and T_0 in our model can be determined with a few *ab initio* simulations or experiments. Our model can be used

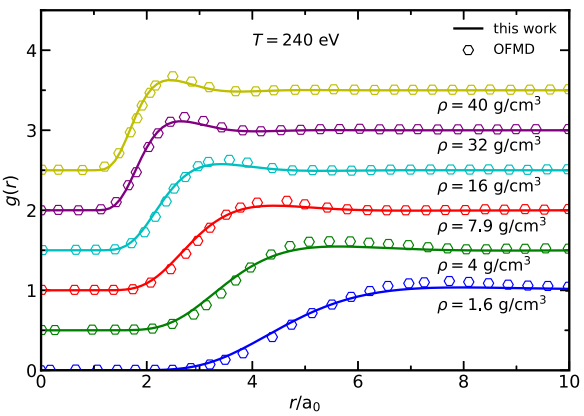

FIG. 4. The RDFs of warm dense Fe at 240 eV with densities from 1.6 g/cm^3 to 40 g/cm^3. The OFMD results are from Ref. [20]. The charge numbers Z calculated by Yukawa model are 16.34, 15.55, 14.99, 14.67, 14.5, 14.59 for ρ=1.6, 4, 7.9, 16, 32, 40 g/cm^3, respectively.

to efficiently calculate the properties of WDM, such as structural information, transport coefficients, and equation of state, over a wide temperature and density range, while *ab initio* simulations typically consume lots of computational time and resources.

ACKNOWLEDGMENTS

This work was supported by the National Natural Science Foundation of China (Grants No. 11575166 and No. 11774321) and CAEP Foundation (Grant No. CX2019023).

[1] T. Guillot, Interiors of giant planets inside and outside the solar system, Science **286**, 72 (1999).

[2] B. Nagler, U. Zastrau, R. R. Fäustlin, S. M. Vinko, T. Whitcher, A. J. Nelson, R. Sobierajski, J. Krzywinski, J. Chalupsky, E. Abreu *et al.*, Turning solid aluminium transparent by intense soft x-ray photoionization, Nat. Phys. **5**, 693 (2009).

[3] P. M. Leguay, A. Lévy, B. Chimier, F. Deneuville, D. Descamps, C. Fourment, C. Goyon, S. Hulin, S. Petit, O. Peyrusse *et al.*, Ultrafast Short-Range Disordering of Femtosecond-Laser-Heated Warm Dense Aluminum, Phys. Rev. Lett. **111**, 245004 (2013).

[4] E. García Saiz, G. Gregori, D. O. Gericke, J. Vorberger, B. Barbrel, R. J. Clarke, R. R. Freeman, S. H. Glenzer, F. Y. Khattak, M. Koenig *et al.*, Probing warm dense lithium by inelastic X-ray scattering, Nat. Phys. **4**, 940 (2008).

[5] A. L. Kritcher, P. Neumayer, J. Castor, T. Döppner, R. W. Falcone, O. L. Landen, H. J. Lee, R. W. Lee, E. C. Morse, A. Ng *et al.*, Ultrafast x-ray Thomson scattering of shock-compressed matter, Science **322**, 69 (2008).

[6] R. Betti and O. A. Hurricane, Inertial-confinement fusion with lasers, Nat. Phys. **12**, 435 (2016).

[7] D. Riley, N. C. Woolsey, D. McSherry, I. Weaver, A. Djaoui, and E. Nardi, X-Ray Diffraction from a Dense Plasma, Phys. Rev. Lett. **84**, 1704 (2000).

[8] S. H. Glenzer, G. Gregori, R. W. Lee, F. J. Rogers, S. W. Pollaine, and O. L. Landen, Demonstration of Spectrally Resolved X-Ray Scattering in Dense Plasmas, Phys. Rev. Lett. **90**, 175002 (2003).

[9] S. H. Glenzer, O. L. Landen, P. Neumayer, R. W. Lee, K. Widmann, S. W. Pollaine, R. J. Wallace, G. Gregori, A. Höll, T. Bornath *et al.*, Observations of Plasmons in Warm Dense Matter, Phys. Rev. Lett. **98**, 065002 (2007).

[10] S. H. Glenzer and R. Redmer, X-ray Thomson scattering in high energy density plasmas, Rev. Mod. Phys. **81**, 1625 (2009).

[11] A. L. Kritcher, P. Neumayer, C. R. D. Brown, P. Davis, T. Döppner, R. W. Falcone, D. O. Gericke, G. Gregori, B. Holst, O. L. Landen *et al.*, Measurements of Ionic Structure in Shock Compressed Lithium Hydride from Ultrafast X-Ray Thomson Scattering, Phys. Rev. Lett. **103**, 245004 (2009).

[12] B. Barbrel, M. Koenig, A. Benuzzi-Mounaix, E. Brambrink, C. R. D. Brown, D. O. Gericke, B. Nagler, M. Rabec le Gloahec, D. Riley, C. Spindloe *et al.*, Measurement of Short-Range Correlations in Shock-Compressed Plastic by Short-Pulse X-Ray Scattering, Phys. Rev. Lett. **102**, 165004 (2009).

[13] T. Ma, T. Döppner, R. W. Falcone, L. Fletcher, C. Fortmann, D. O. Gericke, O. L. Landen, H. J. Lee, A. Pak, J. Vorberger *et al.*, X-Ray Scattering Measurements of Strong Ion-Ion Correlations in Shock-Compressed Aluminum, Phys. Rev. Lett. **110**, 065001 (2013).

[14] L. B. Fletcher, H. J. Lee, T. Döppner, E. Galtier, B. Nagler, P. Heimann, C. Fortmann, S. LePape, T. Ma, M. Millot *et al.*, Ultrabright x-ray laser scattering for dynamic warm dense matter physics, Nat. Photonics **9**, 274 (2015).

[15] A. Denoeud, A. Benuzzi-Mounaix, A. Ravasio, F. Dorchies, P. M. Leguay, J. Gaudin, F. Guyot, E. Brambrink, M. Koenig, S. Le Pape *et al.*, Metallization of Warm Dense SiO_2 Studied by XANES Spectroscopy, Phys. Rev. Lett. **113**, 116404 (2014).

[16] A. Benuzzi-Mounaix, F. Dorchies, V. Recoules, F. Festa, O. Peyrusse, A. Levy, A. Ravasio, T. Hall, M. Koenig, N. Amadou *et al.*, Electronic Structure Investigation of Highly Compressed Aluminum with K Edge Absorption Spectroscopy, Phys. Rev. Lett. **107**, 165006 (2011).

[17] Y. Zhao, J. Yang, J. Zhang, G. Yang, M. Wei, G. Xiong, T. Song, Z. Zhang, L. Bao, B. Deng *et al.*, K-Shell Photoabsorption Edge of Strongly Coupled Matter Driven by Laser-Converted Radiation, Phys. Rev. Lett. **111**, 155003 (2013).

[18] Y. Zhao, Z. Zhang, B. Qing, J. Yang, J. Zhang, M. Wei, G. Yang, T. Song, G. Xiong, M. Lv *et al.*, K-Shell Photoabsorption Edge of Strongly Coupled Aluminum Driven by Laser-Converted Radiation, Europhys. Lett. **117**, 65001 (2017).

[19] K. Wünsch, J. Vorberger, and D. O. Gericke, Ion structure in warm dense matter: Benchmarking solutions of hypernetted-chain equations by first-principle simulations, Phys. Rev. E **79**, 010201(R) (2009).

[20] H. Sun, D. Kang, Y. Hou, and J. Dai, Transport properties of warm and hot dense iron from orbital free and corrected Yukawa potential molecular dynamics, Matter Radiat. Extremes **2**, 287 (2017).

[21] F. Lambert, J. Clérouin, and G. Zérah, Very-high-temperature molecular dynamics, Phys. Rev. E **73**, 016403 (2006).

[22] N. M. Gill, R. A. Heinonen, C. E. Starrett, and D. Saumon, Ion-ion dynamic structure factor of warm dense mixtures, Phys. Rev. E **91**, 063109 (2015).

[23] C. Mo, Z. Fu, W. Kang, P. Zhang, and X. T. He, First-Principles Estimation of Electronic Temperature from X-Ray Thomson Scattering Spectrum of Isochorically Heated Warm Dense Matter, Phys. Rev. Lett. **120**, 205002 (2018).

[24] J. Dai, D. Kang, Z. Zhao, Y. Wu, and J. Yuan, Dynamic Ionic Clusters with Flowing Electron Bubbles from Warm to Hot Dense Iron Along the Hugoniot Curve, Phys. Rev. Lett. **109**, 175701 (2012).

[25] J. Dai, Y. Hou, and J. Yuan, Unified First Principles Description from Warm Dense Matter to Ideal Ionized Gas Plasma: Electron-Ion Collisions Induced Friction, Phys. Rev. Lett. **104**, 245001 (2010).

[26] H. R. Rüter and R. Redmer, *Ab Initio* Simulations for the Ion-Ion Structure Factor of Warm Dense Aluminum, Phys. Rev. Lett. **112**, 145007 (2014).

[27] R. J. Magyar, S. Root, K. Cochrane, T. R. Mattsson, and D. G. Flicker, Ethane-xenon mixtures under shock conditions, Phys. Rev. B **91**, 134109 (2015).

[28] R. Armiento and A. E. Mattsson, Functional designed to include surface effects in self-consistent density functional theory, Phys. Rev. B **72**, 085108 (2005).

[29] A. E. Mattsson, P. A. Schultz, M. P. Desjarlais, T. R. Mattsson, and K. Leung, Designing meaningful density functional theory calculations in materials science—a primer, Modell. Simul. Mater. Sci. Eng. **13**, R1 (2004).

[30] C. E. Starrett, J. Daligault, and D. Saumon, Pseudoatom molecular dynamics, Phys. Rev. E **91**, 013104 (2015).

[31] C. E. Starrett and D. Saumon, Equation of state of dense plasmas with pseudoatom molecular dynamics, Phys. Rev. E **93**, 063206 (2016).

[32] J. Chihara, Y. Ueshima, and S. Kiyokawa, Nucleus-electron model for states changing from a liquid metal to a plasma and the Saha equation, Phys. Rev. E **60**, 3262 (1999).

[33] C. E. Starrett, D. Saumon, J. Daligault, and S. Hamel, Integral equation model for warm and hot dense mixtures, Phys. Rev. E **90**, 033110 (2014).

[34] C. E. Starrett and D. Saumon, Models of the elastic x-ray scattering feature for warm dense aluminum, Phys. Rev. E **92**, 033101 (2015).

[35] Y. Hou, R. Bredow, J. Yuan, and R. Redmer, Average-atom model combined with the hypernetted chain approximation applied to warm dense matter, Phys. Rev. E **91**, 033114 (2015).

[36] J. Clérouin, P. Arnault, C. Ticknor, J. D. Kress, and L. A. Collins, Unified Concept of Effective One Component Plasma for Hot Dense Plasmas, Phys. Rev. Lett. **116**, 115003 (2016).

[37] J. Vorberger and D. Gericke, Effective ion-ion potentials in warm dense matter, High Energy Density Phys. **9**, 178 (2013).

[38] E. García Saiz, G. Gregori, F. Y. Khattak, J. Kohanoff, S. Sahoo, G. Shabbir Naz, S. Bandyopadhyay, M. Notley, R. L. Weber, and D. Riley, Evidence of Short-Range Screening in Shock-Compressed Aluminum Plasma, Phys. Rev. Lett. **101**, 075003 (2008).

[39] J. Vorberger, Z. Donko, I. M. Tkachenko, and D. O. Gericke, Dynamic Ion Structure Factor of Warm Dense Matter, Phys. Rev. Lett. **109**, 225001 (2012).

[40] R. Bredow, T. Bornath, W. Kraeft, M. Dharma-Wardana, and R. Redmer, Classical-map hypernetted chain calculations for dense plasmas, Contrib. Plasma Phys. **55**, 222 (2015).

[41] B. L. Sherman, H. F. Wilson, D. Weeraratne, and B. Militzer, Ab initio simulations of hot dense methane during shock experiments, Phys. Rev. B **86**, 224113 (2012).

[42] D. Kremp, M. Schlanges, and W.-D. Kraeft, *Quantum Statistics of Nonideal Plasmas* (Springer, Berlin, 2013), p. 22.

[43] L. Pauling, The sizes of ions and the structure of ionic crystals, J. Am. Chem. Soc. **49**, 765 (1927).

[44] R. Shannon, Revised effective ionic radii and systematic study of inter atomic distances in halides and chalcogenides, Acta Crystallogr. A **32**, 751 (1976).

[45] D. Wu, S. Lu, and J. Lu, Hydrogen-like calculation formula for cation radius, Chinese Science Bulletin **32**, 195 (1987).

[46] A. K. Verma, P. Modak, and B. B. Karki, First-principles simulations of thermodynamical and structural properties of liquid Al_2O_3 under pressure, Phys. Rev. B **84**, 174116 (2011).

[47] G. Gregori, S. H. Glenzer, W. Rozmus, R. W. Lee, and O. L. Landen, Theoretical model of x-ray scattering as a dense matter probe, Phys. Rev. E **67**, 026412 (2003).

[48] O. Peyrusse, Theoretical calculations of K-edge absorption spectra in warm dense Al, J. Phys. Condens. Matter **20**, 195211 (2008).

[49] P. Sainctavit, D. Cabaret, and V. Briois, Multiple scattering theory applied to x-ray absorption near-edge structure, in *Neutron and X-ray Spectroscopy* (Springer Netherlands, Dordrecht, 2006).